ISIJ International, Vol. 49 (2009), No. 8, pp. 1239–1245

Influence of Chemical Composition and Solidification Rate on the Abrasion and Impact Properties of CADI

Sebastián LAINO, Jorge A. SIKORA and Ricardo C. DOMMARCO

Tribology Group–School of Engineering, Universidad Nacional de Mar del Plata, Metallurgy Department, INTEMA-CONICET, Av. J. B. Justo 4302, B7608FDQ Mar del Plata, Argentina. E-mail: slaino@fi.mdp.edu.ar

(*Received on January 13, 2009; accepted on March 10, 2009*)

The use of CADI, a variant of Austempered Ductile Iron (ADI) containing free carbides, is on the increase thanks to its excellent combination of high abrasion resistance and good impact toughness, when compared to other materials with similar wear resistance.

The present work focuses on the study of two CADI variants in which carbides were obtained by a combination of alloying elements and the effect of a cooper chill located in the mould.

A detailed microstructural characterization of the material was made; and the content and composition of the carbides as well as their stability during the heat treatment were particularly studied. The abrasion wear resistance was evaluated by testing under the ASTM G 65 standard, and comparing the relative wear resistance of samples taken just beside the cooper chill up to locations where the chill did not affect the solidification rate. The relative wear resistance, determined by using ADI as a reference material, ranged from $E \approx 3$ to $E \approx 2$ for samples taken from the different locations, close and far to the chill, respectively. For samples taken from the same locations, the impact toughness ranged from 6.5 to 10 J, respectively. The results allow establishing a relationship between the solidification rate, the microstructure and the mechanical properties, thereby enabling to predict their effect on current applications.

KEY WORDS: CADI; austempering; alloying; chilling effect; microstructure; carbides; abrasive wear; impact toughness.

1. Introduction

Austempered Ductile Iron (ADI) has long been recognized for its high tensile strength and toughness (over 1600 MPa and 110 J for the 1600-1300-01 and 750-500-11 grades respectively, according to the ASTM A 897M-06 standard), which has led to its replacing forged steels in many applications. The optimum performance of ADI under different wear mechanisms such as rolling contact fatigue, adhesion and abrasion[1–3] has also been widely recognized. On the other hand, completely ausferritic matrices have proved to behave in a different manner under abrasive conditions, depending on the tribosystem (low or high stress abrasion), though always ensuring a good performance in service if the heat treatment parameters are properly selected.[2]

Some parts made of gray or ductile irons, either with or without heat treatment, are used for abrasive environments, reinforcing the microstructure with free carbides. Carbidic Austempered Ductile Iron (CADI) constitutes a new type of material recently introduced in the market. The scarce literature available on CADI only provides application examples and data about its response to abrasive wear, though not about its fabrication procedure.

The presence of carbides is expected to promote an increase in the abrasive wear resistance, though a decrease in toughness. Therefore, the challenge in the development of CADI lies in controlling microstructure so as to reach an optimum balance between abrasion resistance and toughness for a given application, *i.e.* taking into account the tribosystem.

A reduction in the quantity of graphitizing elements in ductile iron (in particular Si) is also known to promote the precipitation of ledeburitic carbides during solidification. This methodology may be combined with a second option given by the high undercooling resulting from the use of a chill in the mould. A third option is to alloy the melt with carbide stabilizing elements, such as Cr, Mo or Ti,[4,5] which strongly reduces the interval between stable and metastable eutectic temperatures leading to total or partial solidification according to the metastable diagram.[6]

The undercooling degree affects not only the size and morphology of the solidification structure but also the microsegregation phenomenon. In fact, as solidification advances, the remaining melt becomes enriched in carbide stabilizing alloy elements and impoverished in graphite forming elements. Hence, the lower the cooling rate the greater the microsegregation tendency, thereby increasing the probability for carbide precipitation at the latest stages of solidification taking place in the last to freeze (LTF) zones, forming alloyed carbides (also called intercellular carbides). Accordingly, the size and composition of carbides may vary, from low alloyed cementite to high alloyed carbides, depending on the chemical composition of the

heat and the cooling rate imposed during solidification.[6–9)]

As already demonstrated,[10,11)] ledeburitic carbides, produced by controlling either the cooling rate or the silicon content (non-alloyed carbides), have a great tendency to dissolve during the austenitizing stage of the heat treatment and are less stable than alloyed carbides are. Therefore, if the cast parts need to be heat treated, carbide dissolution during the austenitizing step must be taken into account.

In a previous work by the authors,[12)] CADI with different amounts of carbides obtained by using 1<%Cr<2.5 as their main alloying element, yielded carbide contents ranging from 5 to 21%. Most carbides were found to be stable during the austenitizing stage of the austempering process, and the amount of dissolved carbides was very low or negligible. It was further detected that the impact toughness decreased as the amount of Cr increased, though reaching a quasi-steady level at ~7 J for a CADI alloyed with %Cr>1.5. With regard to impact toughness, the CADI variant alloyed with 1% Cr and austempered at 360°C yielded the highest values in Charpy tests (~25 J). On the other hand, the highest wear resistance was obtained for a CADI alloyed with 2.5% Cr and austempered at T_a=280°C. With respect to the two austempering temperatures evaluated (T_a=280 and 360°C), the CADI samples alloyed with 1.5% Cr, with 2.0% Cr (austempered at T_a=360°C), and with 1% Cr (austempered at T_a=280°C) achieved a good balance between wear resistance and impact toughness.

The present work studies the influence of Cr content, carbon equivalent and chilling effect on the characteristics of CADI's microstructure. It also explores its wear resistance and impact toughness. Said characteristics are evaluated as a function of the distance to a copper chill located in the mould, *i.e.* at different cooling rates.

2. Experimental Procedure

2.1. Material and Sample Preparation

Three ductile iron heats were obtained in a metal casting laboratory using a 55 kg capacity 3 kHz induction furnace. Steel scrap and foundry returns were used as charge materials. Two heats were used to produce CADI samples. One of them was hypoeutectic while the other nearly eutectic. Both were alloyed with Cr to favor the precipitation of alloyed cementite $(Fe, Cr)_3C$.

The shape and dimensions of the model used to make the moulds for casting[13,14)] are shown in **Fig. 1**(a). A copper chill of 38×38×200 mm was located at the end of the plate in order to promote a chilling effect in its vicinity, thus introducing a cooling rate gradient along the plate. The plate was cut as shown in Fig. 1(b), with a longitudinal slice ~80 mm long obtained for microstructural characterization and hardness measurement. Slices of about 12 mm thick and parallel to the cooper chill were also obtained (Figs. 1(a) and 1(b)), and used for impact and wear test samples preparation.

A third unalloyed heat was cast in 25 mm Y Blocks (ASTM A 395) to obtain conventional ADI samples used as reference material for abrasion and impact tests.

All the heats were nodulized with Fe–Si–Mg (9 wt% Mg), inoculated with Fe–Si (75 wt% Si) and alloyed with small amounts of copper and nickel so as to provide enough austemperability.

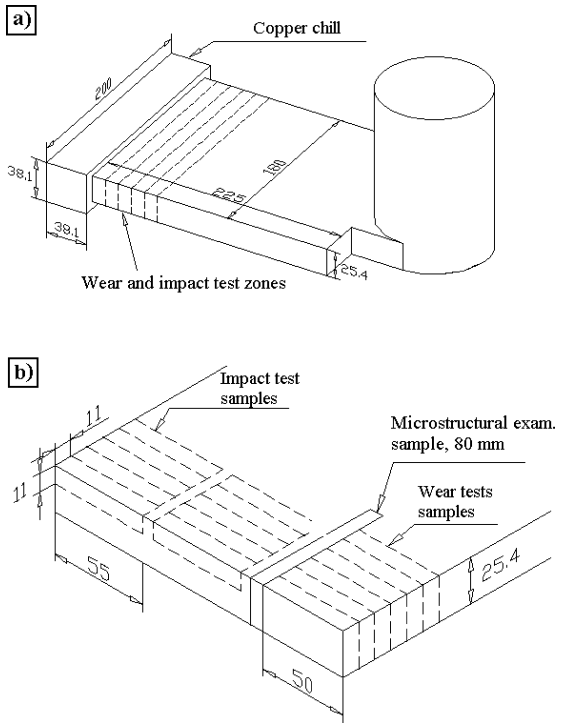

Fig. 1. (a) Plate model with a copper chill, showing the location where the slices for samples preparation were taken. (b) Detail of the location where test samples were obtained.

Table 1. Sample identification and condition (austenitizing temperature T_γ=900°C in all samples).

Heat	Sample identification	Sample condition
1	C1	As-cast
	CADI 1	Austempered (Ta=320 ºC)
2	C2	As-cast
	CADI 2	Austempered (Ta=320 ºC)
3	ADI	Austempered (Ta=320 ºC)

CADI samples were obtained from the two heats alloyed with Cr after a heat treatment involving an austenitizing stage at T_γ=900°C in a muffle during t_γ=1 h, followed by an austempering step in a salt bath at T_a=320°C during t_a=2 h. Conventional ADI samples (used as reference material) were obtained from the Y Blocks of the unalloyed heat by using the same austenitizing and austempering cycles. Sample identification, depending on the heat and heat treatment cycle, is given in **Table 1**.

2.2. Chemical and Microstructural Examination

The chemical composition of the alloys was measured by means of a spark emission optic spectrometer with a DV6 excitation source.

Metallographic sample preparation for optical microscopy examination was conducted by using standard cutting and polishing techniques, and etching with 2% Nital. The amount of carbides *versus* the distance to the chill was measured by using a software for image analysis. For this purpose, carbides were revealed by etching with 10% ammonium persulfate in aqueous solution. The magnification used to obtain data from a sufficiently large area was X50. Each reported value is the average of three measurements

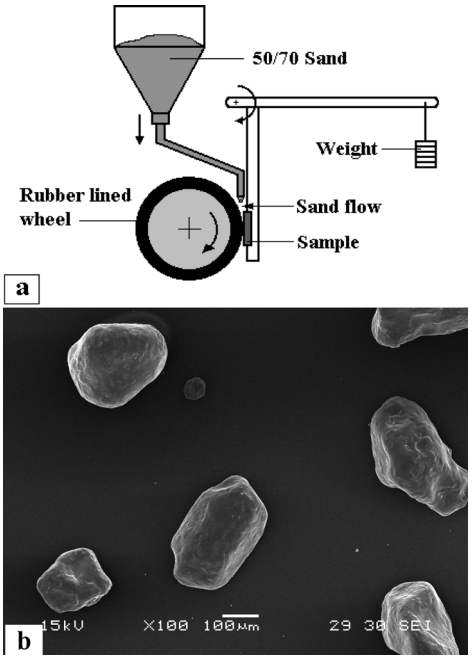

Fig. 2. (a) Schematic of the ASTM G 65 dry sand—rubber wheel abrasion test. (b) SEM photograph of the rounded 50/70 sand grains used in the abrasion test.

taken close to the central line of the plate.

The chemical composition of the carbides was measured at different distances to the chill as a way to evaluate the microsegregation characteristics and its stability during the austenitizing stage of the heat treatment. Compositions were determined by means of a scanning electron microscope with an EDS module, and the reported values are the average of three determinations.

2.3. Mechanical Tests

Brinell hardness was measured in a bench tester using a 2.5 mm tungsten carbide ball and a 187.5 kg load ($HBW_{2.5/187.5}$). A hardness profile as a function of the distance to chill was obtained for each alloy. In order to determine the hardness of the carbides and the matrix separately, microindentation tests were carried out by using a Vickers indenter and a 200 g load (HV_{200}).

The abrasion wear resistance was evaluated by applying the "Dry Sand/Rubber Wheel Abrasion Test" (**Fig. 2**(a)) according to the ASTM G 65 standard, and using the procedure A (test load 130 N, number of wheel revolutions 6 000). The Relative Wear Resistance index, E, was obtained as the ratio between the volume loss experienced by the ADI samples, used as reference material (ΔV_R), and the CADI samples (ΔV_S), according to Eq. (1). The weight loss values were measured by means of a 0.1 mg precision scale and then converted into volume loss by using the material's density measured on calibrated blocks made from all the alloys and taken at different distances to the chill.

$$E = \frac{\Delta V_R}{\Delta V_S}$$

Figure 2(b) shows a SEM photograph of the sand grains used in the ASTM G 65 wear test, with their rounded shape and with an average typical diameter of ~200 mm, as determined by the standard.

Table 2. Chemical composition of the heats [weight %].

Heat	C	Si	S	P	Cu	Ni	Cr	CE
1	3.20	1.97	0.04	0.05	0.66	0.66	0.43	3.85
2	3.40	3.00	0.02	0.03	0.65	0.56	2.04	4.40
3	3.40	3.34	0.02	0.03	0.62	0.63	0	4.51

Impact toughness tests on ADI and CADI samples were carried out in agreement with the ASTM E 23 standard using 10×10×55 mm specimens and an Amsler pendulum with an initial energy of 300 J (5 m/s impact speed). In view of the characteristics of the materials evaluated, unnotched samples were employed. The reported values are the average of four determinations.

3. Results and Discussion

3.1. Chemical and Microstructural Characterization

Table 2 lists the chemical compositions of the heats. It should be noted that heat 1 was hypoeutectic (CE=3.85%) and alloyed with 0.43% Cr, whereas heat 2 was nearly eutectic (CE=4.40%) and alloyed with 2.04% Cr. Both heats were alloyed with chromium in order to promote partial solidification according to the Fe–C metastable diagram. This, in addition to the microsegregation effect, led to alloyed eutectic carbides formation.

Figures 3 and **4** show the microstructures of heats 1 and 2 after austempering (samples CADI 1 and 2, respectively), at different distances to the chill (d). It can be observed that there is a high concentration of small carbides close to the chill (d~0 mm), as well as a high amount of small graphite nodules, typically of about 10–15 μm in diameter. As d increases, fewer carbides, a lower nodule count and a larger nodule size is observed. It can also be noticed that the carbide size increases. In all cases, the matrix was fully ausferritic exhibiting the typical morphology corresponding to the intermediate austempering temperature (T_a=320°C) used in the present study.

Figures 5(a) and 5(b) depict the carbide content as a function of the distance to the chill, measured under both as cast (C1 and C2) and heat treated (CADI 1 and CADI 2) conditions. It should be noticed that the carbide content in sample C1 was higher than that in sample C2 at all distances to the chill, even though the average chromium content in C1 was lower than that in C2. This result clearly demonstrates the effect of the hypoeutectic composition of heat 1, *i.e.* the lower silicon level. Then, the graphitizing potential seems to be a dominant parameter controlling carbide formation.

In Fig. 5(a), it can be further observed that the carbide content in sample C1 decreases after the heat treatment cycle (CADI 1) for all distances to the chill, owing to its partial dissolution which occurs at the austenitizing temperature (T_γ). The dissolution degree was maximum at d=0 (about 45%), decreasing as the distance to the chill increased, up to reaching very low values (~5%), in which case the chill no longer affected the solidification rate. On the other side, the carbide content in sample C2 remains mostly unchanged after the heat treatment (CADI 2), Fig. 5(b), for all distances to chill.

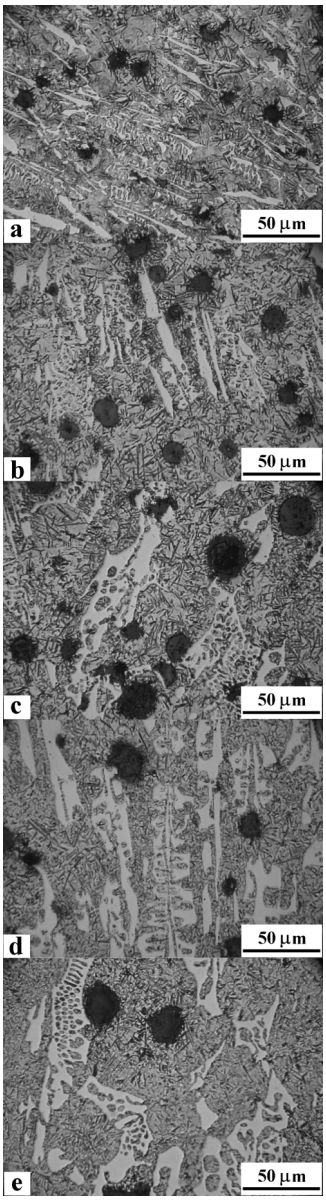

Fig. 3. Microstructures of CADI 1 samples austempered at T_a=320°C. Distance to chill [mm], (a) 0, (b) 10, (c) 20, (d) 40, and (e) 60.

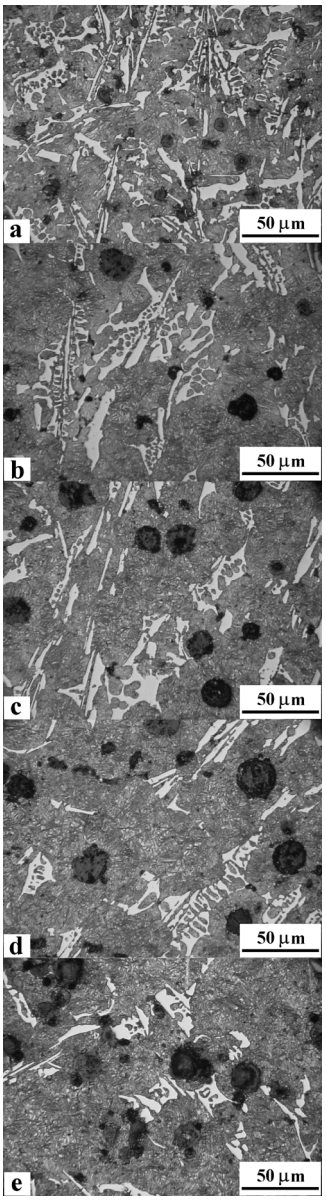

Fig. 4. Microstructures of CADI 2 samples austempered at T_a=320°C. Distance to chill [mm], (a) 0, (b) 10, (c) 20, (d) 40, and (e) 60.

As the main alloying element to promote carbide precipitation was Cr, an EDS semi-quantitative analysis of the Cr content in the carbides *versus d* was performed. The values are reported in **Fig. 6**, and yield noticeably higher levels than the alloy average (Cr_0), due to the microsegregation effect. In CADI 1, the Cr content in the carbides at d=0 mm was four times the Cr_0, (Cr=2%), while in CADI 2 it was twice the Cr_0, (Cr=4%). For both alloys, these values increased with d as the solidification rate decreased, which, in turn, made microsegregation increase. For CADI 1, the Cr content increased up to 3% and for CADI 2 up to 8%. The results show that, even though it is possible to obtain high carbide content by decreasing the average Cr in a hypoeutectic alloy, this leads to carbides formation that may partially dissolve during the austenitizing stage.

Therefore, carbides in C1 have less chromium than those in C2, particularly close to the chill, making them less stable at T_γ. For this reason, the maximum carbide dissolution was observed in CADI 1 close to the chill, where the microsegregation effect was minor and the carbides Cr content the lowest (see Fig. 5). As the distance to the chill increased, microsegregation became more significant, increasing carbides chromium content and turning it more stable during the austenitizing, thereby resulting in a lower dissolution degree. These results are consistent with those derived from a previous work.[12)]

The EDS semi-quantitative analysis also included a Cr mapping. **Figure 7**(a) shows the microstructure of a CADI 1 sample and Fig. 7(b) shows the Cr mapping for the same region. A much higher Cr content is noticed in the carbides than in the matrix. The Cr content in the ausferrite matrix was also determined by EDS for both alloys, at a region far from the chill. The results showed that the Cr content in the matrix was about half the Cr_0 (0.26% and 0.92% for CADI 1 and CADI 2, respectively).

3.2. Mechanical Tests

For abrasive purposes, hardness is usually a key factor.

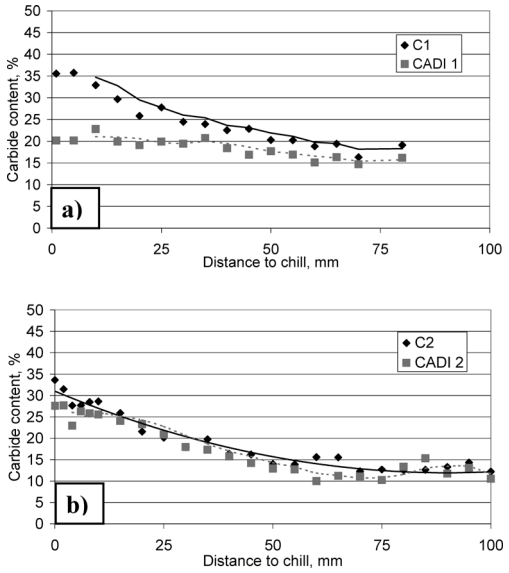

Fig. 5. Carbide content in as cast samples (C1, C2) and austempered samples (CADI 1, CADI 2) at different distances to the chill.

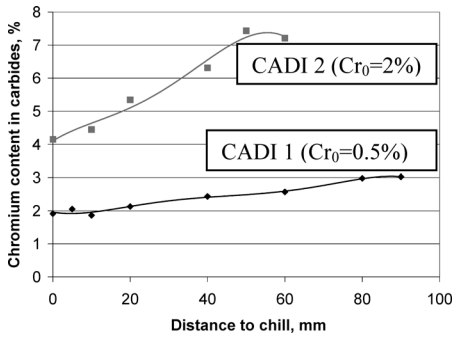

Fig. 6. EDS semi quantitative analysis for the Cr content in carbides of heats 1 and 2 at different distances to the chill. Average Cr content for heats 1 and 2 was 0.43% and 2.04%, respectively.

Nevertheless, in reinforced materials there are many other variables which also play a part in the final response to abrasive wear. It is well known that the hardness of a multiphase material can be attributed to the hardness of the individual microconstituents as well as to their relative amount, shape, size, orientation and distribution. In this case, the hardness of the microconstituents was 442 HV_{200} for the ausferritic matrix and 1 100 HV_{200} for the carbides, as determined by the microindentation tests. The influence of the amount of reinforcing particles (carbides) was reflected in the hardness profile as a function of d, **Fig. 8**.

As noted from Figs. 5 and 8, the decrease in carbide content as d increases promotes hardness decrease for both heats, and the hardness profiles reach a stable value at a distance in which the carbide content also stabilizes ($d>$ 75 mm).

To calculate the relative wear resistance (E) accurately, it is necessary to know the material's density so as to obtain the volume loss values from the weight loss measured after the abrasion tests. Considering that the variable cooling rates at the different plate locations affect the microstructure and hence the material's density, this characteristic was measured at different distances from the chill for CADI 1

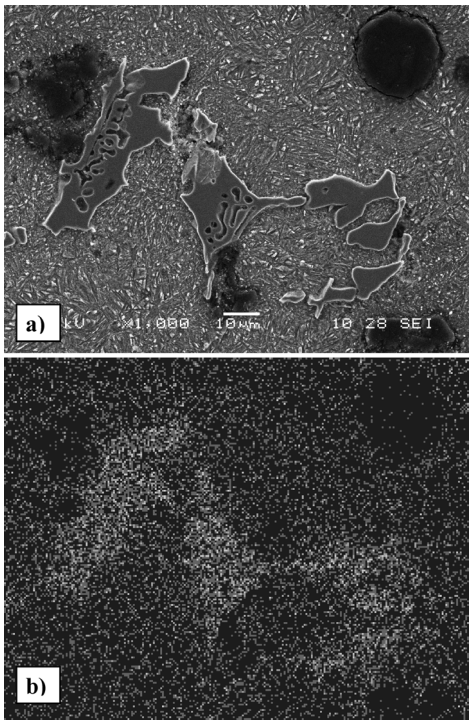

Fig. 7. EDS Cr mapping. (a) CADI 1 microstructure, and (b) Cr distribution.

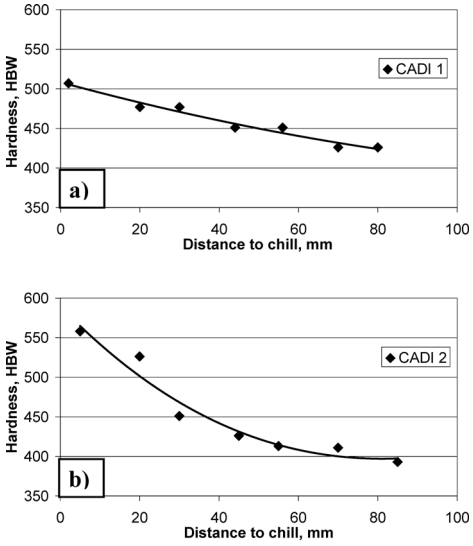

Fig. 8. Hardness values *versus* distance to the chill of CADI samples.

and 2, using 10×10×25 mm ground calibrated blocks. Results are indicated in **Fig. 9**. The density of heat 3, used to produce the conventional ADI, was 7.09 g/cm^3, due to the higher graphite content in comparison with the CADI samples. In order to validate the accuracy of the used method, the density of a SAE 1010 block was also measured, yielding 7.71 g/cm^3.

Figure 10 shows the abrasion test results for CADI 1 and 2, reported as volume loss values *versus d*. These results are also presented in **Table 3** in terms of the relative wear resistance index (E) *versus d*. The unexpected behavior of CADI 1 close to the chill was attributed to the presence of cast defects macroscopically observed in this region, due to the extremely high cooling rate. These defects act as wear

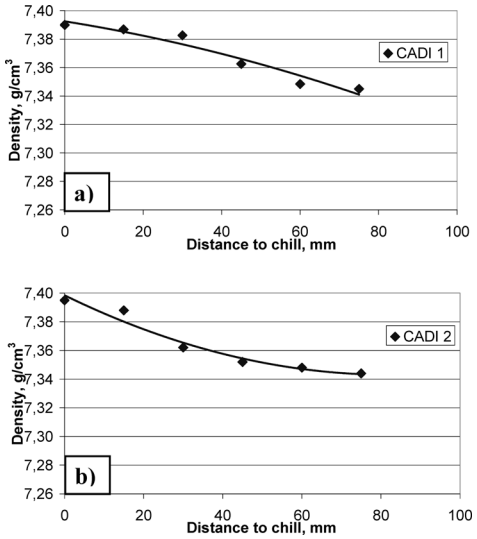

Fig. 9. Density values as a function of the distance to the chill for CADI samples.

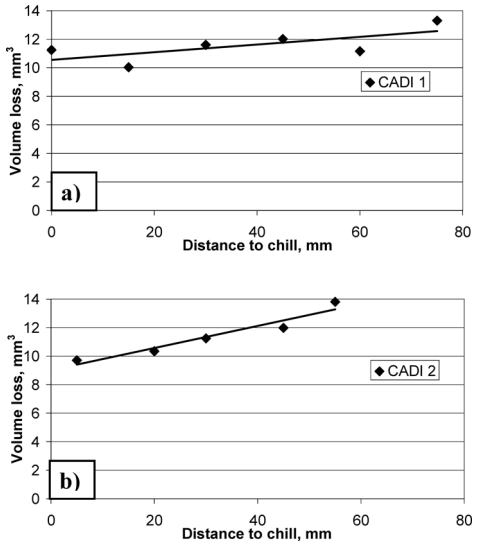

Fig. 10. Volume loss values *versus* distance to the chill for CADI samples (the average volume loss for the ADI 320 used as reference material was 30.2 mm^3).

Table 3. Relative wear resistance (*E*) values for CADI 1 and CADI 2 samples, at different distances to the chill (reference material, ADI).

Distance to the chill [mm]	Relative wear resistance – E	
	CADI 1	CADI 2
0	2.68	3.11
15	3.01	2.92
30	2.60	2.69
45	2.58	2.52
60	2.75	2.19
75	2.27	-

concentrators. For the rest of the evaluated zones of CADI 1 and CADI 2, the abrasion resistance slightly decreased as *d* increased. It should be pointed out that, regarding the tribosystem evaluated in this work, the wear resistance increased as hardness did. Yet this behavior may not replicate when other tribosystems are considered.

The effectiveness of carbides as reinforcing particles is

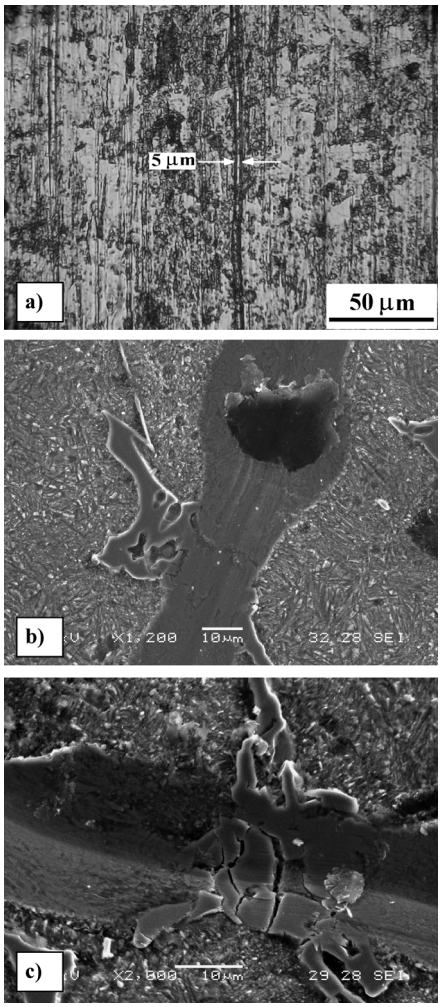

Fig. 11. Wear scars produced on a CADI sample. (a) ASTM G 65 wear test, (b) scratch made with a Vickers indenter using a 100 g load, and (c) detail of carbide fracture during scratching.

mainly determined by the size relationship between the scratch width and depth; also by the size, the volume fraction, the distance and other characteristics of the carbides.[15] The wear scar of a laboratory test sample is shown in **Fig. 11**(a), with parallel scratches with a width of up to ~5 μm. The size of the scratches is comparable to the size of the microconstituents and also to the distance between carbides (Figs. 3 and 4), thereby demonstrating that the average distance between carbides is sometimes greater and sometimes lesser than the groove size. Then, under this testing condition, the maximum reinforcing effect of the carbides is obtained for the microstructure solidified close to the chill, in which the carbide volume fraction is the highest and the distance between carbides is the least.

Figure 11(b) shows the variable size of a ~20 μm wide scratch made with a Vickers indenter (employing a 100 g load) on a polished and etched surface. Indeed, when the indenter travels over the graphite nodule, the width is the largest, while when on the matrix or the carbide the width is the shortest.

However, it should be considered that carbides may also be fractured when scratched by an abrasive particle or traveling indenter, as shown in Fig. 11(c), where portions of the carbide appear to be ready to detach at the following

scratch.

Somehow, the size of the scratches characterizes the severity of the abrasive process. For the ASTM G 65 test conditions, the abrasion severity is low and the presence of carbides really works as a reinforcing element. Nevertheless, if the abrasive process scratches or severity increases, the presence of carbides may be detrimental. This was observed in field tests carried out by the authors on CADI load bucket protection segments, in which the size of the microconstituents was similar to that in the present study, but the scratches were ~100–200 μm wide. In this case, the wear resistance was lower than that of the conventional ADI used as a reference material, being $E\sim0.95$ and $E\sim0.7$ for two CADI variants alloyed with 1.0 and 2.0% Cr, respectively.

The reinforcing effect of the carbides on the wear resistance of the studied materials is indicated in Table 3, showing that the reference material wears at a rate three times faster than the CADI variants ($E\sim3$ at $d=0$ mm for CADI 1 and CADI 2). Then, as d increases, the reduction of carbide content also leads to a decrease in the abrasion resistance, reaching stabilized values for regions where the carbide content was minimum and constant ($d>75$ mm).

Figure 12 reports the impact test results for the CADI obtained in this study, in terms of impact toughness *versus* distance to chill. Both CADI variants have impact toughness values of about 6 J at $d=0$ mm, in accordance with the highest carbide contents, and increasing with d up to values of about 10 J at $d>60$ mm, in accordance with the lowest carbide contents.

Notwithstanding carbides work as reinforcing elements in terms of abrasion resistance (as shown above), their presence negatively affects the impact toughness of CADI, considering the fact that austempered ductile irons have a minimum impact toughness of 20 and 110 J for grades 1600-1300-01 and 750-500-11, respectively, according to the ASTM A 897M. Nevertheless, it is important to point out that the impact toughness of CADI turned out to be greater than that of white irons or carbidic ductile irons with martensitic or pearlitic matrices.

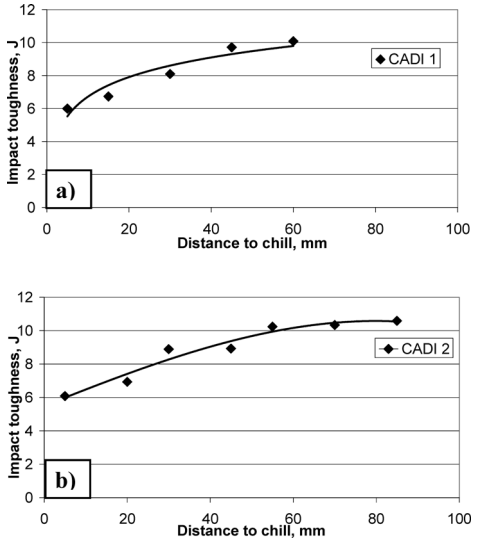

Fig. 12. Impact toughness *versus* distance to the chill for CADI samples.

4. Conclusions

Similar variants of CADI were obtained by different manufacturing processes, combining the chilling and alloying effects in different ways. The characteristics and composition of the carbides under as cast conditions depend on the processing parameters (*i.e.* carbon equivalent, alloying content, cooling rate, *etc.*), which in turn rule the carbide dissolution level at the austenitizing temperature. It was also observed that the less alloyed carbides were, the greater their dissolution level was.

The effectiveness of carbides as reinforcing particles with respect to hardness depends mainly on their volume fraction, *i.e.* the greater the carbide content, the greater the hardness. On the other hand, if the carbides are considered to act as reinforcing particles for abrasion applications, their effectiveness also depends on the relationship between the size of the scratch width and depth, and the size and distribution of the carbides. Then, if the distance between carbides is lesser than the scratch width is, the reinforcing effect turns out to be markedly high. This was observed for the microstructures solidified close to the chill under the laboratory testing conditions used in this work.

Moreover, it was noted that the carbide wear process was dominated by its fracture when scratched by an abrasive particle.

The presence of carbides in ductile iron negatively affects its impact toughness. Nevertheless, the impact toughness of CADI results significantly greater if compared to that of other materials used in the same wear environments, *i.e.* white cast irons of similar hardness.

REFERENCES

1) L. Magalhães and J. Seabra: *Wear*, **215** (1998), 237.
2) R. Dommarco, I. Galarreta, H. Ortiz, P. David and G. Maglieri: *Wear*, **249** (2001), 101.
3) R. Dommarco and J. Salvande: *Wear*, **254** (2003), 230.
4) J. R. Keough and K. L. Hayrynen: *Ductile Iron News*, **3** (2000).
5) K. L. Hayrynen and K. R. Brandenberg: *American Foundry Society*, **111** (2003), 845.
6) R. B. Gundlach, J. F. Janowak, S. Bechet and K. Rohrig: Materials Research Society Symp. Proc., Vol. 34, ed. by H. Fredriksson and M. Hillert, North-Holland, (1985), 251.
7) J. Lacaze, G. Torres Camacho and C. Bak: *Int. J. Cast Met. Res.*, **16** (2003), 167.
8) L. Nastac and D. M. Stefanescu: *Adv. Mater. Res.*, **4–5** (1997), 469.
9) H. Zhao and B. Liu: *ISIJ Int.*, **41** (2001), 986.
10) A. Giacopini, R. Boeri and J. Sikora: *Mater. Sci. Technol.*, **19** (2003), No. 12, 1755.
11) M. Caldera, G. Rivera, R. Boeri and J. Sikora: *Mater. Sci. Technol.*, **21** (2005), No. 10, 1187.
12) S. Laino, J. A. Sikora and R. C. Dommarco: *Wear*, **265** (2008), 1.
13) J. Hemanth: *Mater. Sci. Technol.*, **15** (1999), 878.
14) J. Hemanth: *Mater. Des.*, **21** (2000), 139.
15) K. H. Zum Gahr: *Tribol. Int.*, **31** (1998), No. 10, 587.